Unsaturated Cyclopentadienyl-Molybdenum and Tungsten Carbonyl Cluster Complexes Containing Pd- and Pt(PBu^t_3) Groups

Richard D. Adams,* Carl B. Hollandsworth, and Jack L. Smith, Jr.

Department of Chemistry and Biochemistry, University of South Carolina, Columbia, South Carolina 29208

Received February 2, 2006

A series of new bimetallic cluster compounds, $Cp_2M_2(CO)_4[M'(PBu^t_3)]_2$ [M = Mo, M′ = Pt (**9**); M = Mo, M′ = Pd (**10**); M = W, M′ = Pt (**11**); M = W, M′ = Pd (**12**)], have been synthesized from reactions of $[CpM(CO)_3]_2$ (M = Mo, W) with an excess of $M'(PBu^t_3)_2$ (M′ = Pt, Pd) at various temperatures. Each compound was fully characterized by IR, ^1H and ^{31}P NMR, and single-crystal X-ray diffraction analyses. The metal atoms in the structure of **9** are arranged in a butterfly configuration, while the metal atoms of **10**−**12** adopt a tetrahedral geometry. Compounds **9** and **12** contain two edge-bridging and two triply bridging carbonyl ligands, **10** contains four triply bridging carbonyl ligands, and **11** contains two terminal and two edge-bridging carbonyl ligands. Each of the products is electron-deficient and the M−M bonds, M = Mo and W, are short, Mo−Mo = 2.6535(4) Å in **9** and 2.6362(4) Å in **10**, W−W = 2.6168(9) Å in **11** and 2.6320(7) Å in **12**, which is indicative of some localized multibond character between these metal atoms within the cluster framework. The nature of the bonding within the clusters was explored with DFT calculations (ADF 2004.01, PW91) for the title compounds in C_2 symmetry as well as for a hypothetical, two-electron-reduced $[Cp_2Mo_2Pd_2(CO)_4(PBu^t_3)_2]^{2-}$ species.

Introduction

Bimetallic catalysts, especially those containing platinum or palladium, are widely used in the chemical industry for the large-scale production of important organic compounds.[1] Recent studies have shown that bimetallic cluster complexes can be precursors to highly active and selective heterogeneous bimetallic nanoparticle catalysts for hydrogenation when placed on suitable oxide supports.[2] Their superior properties have in some cases been attributed to synergistic interactions between two different types of metal atoms.[3]

Platinum compounds with sterically encumbered phosphine ligands have been used to prepare a variety of unusual bimetallic cluster complexes over the years.[4] Recently, we have shown that the compounds $M'(PBu^t_3)_2$ (M′ = Pt, Pd) readily react with metal carbonyl cluster complexes to form a variety of new bimetallic cluster complexes by transferring $M'(PBu^t_3)$ groups to their metal−metal bonds.[5] These new compounds are generally ligand-deficient and thus electron-deficient because of the steric effects of the bulky PBu^t_3 ligand. For example, $Ru_3(CO)_{12}$ reacts with $Pd(PBu^t_3)_2$ to yield the tripalladium-triruthenium complex $Ru_3(CO)_{12}[Pd(PBu^t_3)]_3$ (**1**), which exhibits a triangulated "raft" structure having a $Pd(PBu^t_3)$ group bridging each of the three Ru−Ru bonds of the original $Ru_3(CO)_{12}$ cluster.

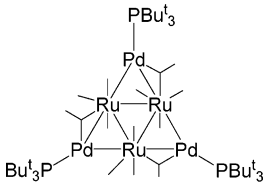

1

Compound **1** has only 84 cluster valence electrons, six electrons less than that expected for a cluster in which all metal atoms obey the 18-electron rule.[5a] $Os_3(CO)_{12}$ reacts similarly with $Pt(PBu^t_3)_2$ at room temperature but yields a series of new

(1) (a) Sinfelt, J. H. *Bimetallic Catalysts. Discoveries, Concepts and Applications*; Wiley: New York, 1983. (b) Sinfelt, J. H. *Sci. Am.* **1985**, *253*, 90. (c) Sinfelt, J. H.; Via, G. H. *J. Catal.* **1979**, *56*, 1. (d) Xiao, J.; Puddephatt, R. J. *Coord. Chem. Rev.* **1995**, *143*, 457. (e) Dees, M. J.; Ponec, V. *J. Catal.* **1989**, *115*, 347. (f) Rice, R. W.; Lu, K. *J. Catal.* **1982**, *77*, 104. (g) Rasser, J. C.; Beindorff, W. H.; Scholten, J. F. *J. Catal.* **1979**, *59*, 211.

(2) (a) Thomas, J. M.; Johnson, B. F. G.; Raja, R.; Sankar, G.; Midgley, P. A. *Acc. Chem. Res.* **2003**, *36*, 20. (b) Raja, R.; Khimyak, T.; Thomas, J. M.; Hermans, S.; Johnson, B. F. G. *Angew. Chem., Int. Ed.* **2001**, *40*, 4638. (c) Hermans, S.; Raja, R.; Thomas, J. M.; Johnson, B. F. G.; Sankar, G.; Gleeson, D. *Angew. Chem., Int. Ed.* **2001**, *40*, 1211. (d) Shephard, D. S.; Maschmeyer, T.; Johnson, B. F. G.; Thomas, J. M.; Sankar, G.; Ozkaya, D.; Zhou, W.; Oldroyd, R. D.; Bell, R. G. *Angew. Chem., Int. Ed. Engl.* **1997**, *36*, 2242. (e) Shephard, D. S.; Maschmeyer, T.; Sankar, G.; Thomas, J. M.; Ozkaya, D.; Johnson, B. F. G.; Raja, R.; Oldroyd, R. D.; Bell, R. G. *Chem. Eur. J.* **1998**, *4*, 12.

(3) (a) Raja, R.; Sankar, G.; Hermans, S.; Shephard, D. S.; Bromley, S.; Thomas, J. M.; Johnson, B. F. G. *Chem. Commun.* **1999**, 1571. (b) Alexeev, O. S.; Gates, B. C. *Ind. Eng. Chem. Res.* **2003**, *42*, 1571. (c) Goodman, D. W.; Houston, J. E. *Science* **1987**, *236*, 403. (d) Ichikawa, M. *Adv. Catal.* **1992**, *38*, 283.

(4) (a) Farrugia, L. J. *Adv. Organomet. Chem.* **1990**, *31*, 301. (b) Farrugia, L. J.; Howard, J. A. K.; Mitrprachachon, P.; Stone, F. G. A.; Woodward, P. *J. Chem. Soc., Dalton Trans.* **1981**, 151.

(5) (a) Adams, R. D.; Captain, B.; Fu, W.; Hall, M. B.; Manson, J.; Smith, M. D.; Webster, C. E. *J. Am. Chem. Soc.* **2004**, *126*, 5253. (b) Adams, R. D.; Captain, B.; Zhu, L. *Inorg. Chem.* **2005**, in press. (c) Adams, R. D.; Captain, B.; Fu, W.; Pellechia, P. J.; Smith, M. D. *Inorg. Chem.* **2003**, *42*, 2094. (d) Adams, R. D.; Captain, B.; Hall, M. B.; Smith, J. L., Jr.; Webster, C. E. *J. Am. Chem. Soc.* **2005**, *127*, 1007. (e) Adams, R. D.; Captain, B. *Angew. Chem., Int. Ed.* **2005**, *44*, 2531. (f) Adams, R. D.; Captain, B.; Pellechia, P. J.; Smith, J. L., Jr. *Inorg. Chem.* **2004**, *43*, 2695. (g) Adams, R. D.; Captain, B.; Fu, W.; Smith, J. L., Jr.; Smith, M. D. *Organometallics* **2004**, *23*, 589. (h) Adams, R. D.; Captain, B.; Fu, W.; Hall, M. B.; Smith, M. D.; Webster, C. E. *Inorg. Chem.* **2004**, *43*, 3921. (i) Adams, R. D.; Captain, B.; Smith, M. D. *J. Cluster Sci.* **2004**, *15*, 139. (j) Adams, R. D.; Captain, B.; Fu, W.; Smith, M. D. *J. Organomet. Chem.* **2003**, *682*, 113. (k) Adams, R. D.; Captain, B.; Pellechia, P. J.; Zhu, L. *Inorg. Chem.* **2004**, *43*, 7243.

10.1021/om060107g CCC: $33.50
Publication on Web 04/04/2006

compounds $Os_3(CO)_{12}[Pt(PBu^t_3)]_n$ [$n = 1$ (**2**), 2 (**3**), and 3 (**4**)], having 1−3 $Pt(PBu^t_3)$ groups bridging the Os−Os bonds of the original $Os_3(CO)_{12}$ complex.[5b]

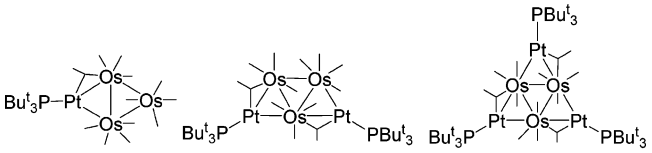

2 **3** **4**

$Ru_5(CO)_{15}(\mu_5\text{-C})$ reacts with $Pt(PBu^t_3)_2$ to yield the adduct $Ru_5(CO)_{15}(C)[Pt(PBu^t_3)]$, which exists as two isomers (**5a** and **5b**) that interconvert rapidly in solution on the NMR time scale.[5c]

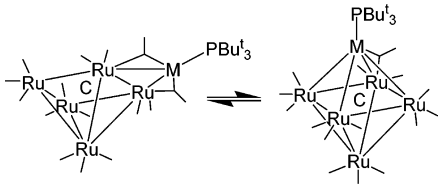

5a **5b**

A bis-$Pt(PBu^t_3)$ adduct of $Ir_4(CO)_{12}$, $Ir_4(CO)_{12}[Pt(PBu^t_3)]_2$ (**6**), was obtained similarly.[5d] By contrast, the reaction of $Pt(PBu^t_3)_2$ with $Re_2(CO)_{10}$ yielded the compound $Pt_3Re_2(CO)_6(PBu^t_3)_3$ (**7**), containing a trigonal bipyramidal structure formed by the insertion of three $Pt(PBu^t_3)$ groups into the Re−Re bond of the $Re_2(CO)_{10}$.[5e] Compound **7** contains only 62 cluster valence electrons, 10 less than the expected number. Interestingly, compound **7** readily reacts with hydrogen at room temperature to form the hexahydride complex $Pt_3Re_2(CO)_6(PBu^t_3)_3(\mu\text{-H})_6$ (**8**), which contains a similar trigonal bipyramidal structure but has a hydrido ligand bridging each of the six Re−Pt bonds in the complex and a total of 68 cluster valence electrons.

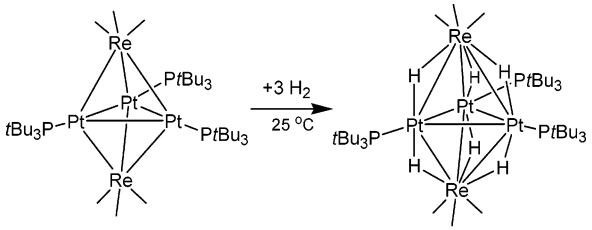

7 **8**

We have now investigated the reaction of $M'(PBu^t_3)_2$ (M' = Pt, Pd) with $[CpM(CO)_3]_2$ (M = Mo, W) and have obtained four new $M_2M'_2$ clusters of the form $Cp_2M_2(CO)_4[M'(PBu^t_3)]_2$ [M = Mo, M' = Pt (**9**); M = Mo, M' = Pd (**10**); M = W, M' = Pt (**11**); M = W, M' = Pd (**12**)]. These compounds are also highly unsaturated electronically. They contain only 54 valence electrons, six electrons less than the number required for tetrahedral tetranuclear metal cluster complexes in which all metal atoms have 18-electron configurations. In this report the synthesis and structures of the new complexes **9**−**12** are described along with some analysis of the M−M bonding aided by DFT computational data.

Experimental Section

General Data. All reactions were performed under a nitrogen atmosphere. Reagent grade solvents were dried by the standard procedures and were freshly distilled prior to use. Infrared spectra were recorded on a Thermo-Nicolet Avatar 360 FT-IR spectrophotometer. All NMR spectra were recorded on a Varian Mercury 400 spectrometer operating at 400.048 MHz. $^{31}P\{^1H\}$ NMR spectra were externally referenced against 85% *ortho*-H_3PO_4. Mass spectrometric measurements performed by direct exposure probe using electron impact ionization (EI) were obtained on a VG 70S instrument. Elemental analyses were performed by Desert Analytics (Tucson, AZ). Product separations were performed by TLC in air on Analtech 0.5 mm silica gel 60 Å F_{254} glass plates. $[CpMo(CO)_3]_2$ and $[CpW(CO)_3]_2$ were purchased from Aldrich Chemical, Co. $Pt(PBu^t_3)_2$ and $Pd(PBu^t_3)_2$ were obtained from Strem.

Synthesis of $Cp_2Mo_2(CO)_4[Pt(PBu^t_3)]_2$ (9). $Pt(PBu^t_3)_2$ (184 mg, 0.305 mmol) was added to a suspension of $[CpMo(CO)_3]_2$ (30 mg, 0.061 mmol) in 25 mL of hexane. The reaction mixture was heated to reflux and stirred for 12 h. After cooling, the solvent was removed in vacuo, and the products were separated by TLC using a 1:1 hexane/methylene chloride solvent mixture to yield 21.7 mg (29%) of green $Cp_2Mo_2(CO)_4[Pt(PBu^t_3)]_2$ (**9**) and 3.6 mg of yellow $Pt_3(CO)_3(PBu^t_3)_3$. Spectral data for **9**: IR ν_{CO} (cm^{-1} in CH_2Cl_2) 1741 (m), 1679 (s); ^1H NMR (CD_2Cl_2 in ppm) δ 5.00 (s, 10 H, C_5H_5), 1.48 (d, 54 H, CH_3, $^3J_{P-H} = 12$ Hz); $^{31}P\{^1H\}$ NMR (CD_2Cl_2 in ppm) δ 109.3 (s, 2 P, $^1J_{Pt-P} = 5987$ Hz). Anal. Calcd: 37.01 C, 5.23 H. Found: 37.06 C, 5.01 H.

Synthesis of $Cp_2Mo_2(CO)_4[Pd(PBu^t_3)]_2$ (10). $Pd(PBu^t_3)_2$ (156 mg, 0.0305 mmol) was added to a suspension of $[CpMo(CO)_3]_2$ (30 mg, 0.061 mmol) in 25 mL of hexane. The reaction mixture was heated to reflux and stirred for 5 h. After cooling, the solvent was removed in vacuo, and the product was separated by TLC using a 1:1 hexane/methylene chloride solvent mixture to yield 26.6 mg (41%) of brown $Cp_2Mo_2(CO)_4[Pd(PBu^t_3)]_2$ (**10**). Spectral data for **10**: IR ν_{CO} (cm^{-1} in CH_2Cl_2) 1747 (m), 1694 (s); ^1H NMR (C_6D_6 in ppm) δ 4.25 (s, 10 H, C_5H_5), 1.46 (d, 54 H, CH_3, $^3J_{P-H} = 12$ Hz); $^{31}P\{^1H\}$ NMR (C_6D_6 in ppm) δ 76.0 (s, 2 P). Anal. Calcd: 43.26 C, 6.12 H. Found: 43.45 C, 5.84 H.

Synthesis of $Cp_2W_2(CO)_4[Pt(PBu^t_3)]_2$ (11). $Pt(PBu^t_3)_2$ (135 mg, 0.225 mmol) was added to a solution of $[CpW(CO)_3]_2$ (30 mg, 0.045 mmol) in 25 mL of toluene. The reaction mixture was heated to reflux and stirred for 3 h. After cooling, the solvent was removed in vacuo, and the product was separated by TLC using a 1:1 hexane/methylene chloride solvent mixture to yield 11.1 mg (18%) of brown $Cp_2W_2(CO)_4[Pt(PBu^t_3)]_2$ (**11**). Spectral data for **11**: IR ν_{CO} (cm^{-1} in CH_2Cl_2) 1802 (m), 1710 (s); ^1H NMR (CD_2Cl_2 in ppm) δ 5.07 (s, 10 H, C_5H_5), 1.49 (d, 54 H, CH_3, $^3J_{P-H} = 12$ Hz); $^{31}P\{^1H\}$ NMR (CD_2Cl_2 in ppm) δ 123.5 (s, 2 P, $^1J_{Pt-P} = 5798$ Hz, $^2J_{Pt-P} = 160$ Hz, $^3J_{P-P} = 97$ Hz,); MS *m*/*e* 1404 (M^+), 1376 ($M^+ - CO$), 1348 ($M^+ - 2CO$), 1003, 950. Anal. Calcd: 32.49 C, 4.59 H. Found: 31.83 C, 4.25 H.

Synthesis of $Cp_2W_2(CO)_4[Pd(PBu^t_3)]_2$ (12). $Pd(PBu^t_3)_2$ (115 mg, 0.225 mmol) was added to a solution of $[CpW(CO)_3]_2$ (30 mg, 0.045 mmol) in 25 mL of benzene. The reaction mixture was heated to reflux and stirred for 1 h. After cooling, the solvent was removed in vacuo, and the product was separated by TLC in air by using a 1:1 hexane/methylene chloride solvent mixture to yield 12.2 mg (22%) of brown $Cp_2W_2(CO)_4[Pd(PBu^t_3)]_2$ (**12**). Compound **12** is air-sensitive. Alternatively, it can also be obtained in a better yield in good purity by removal of the benzene solvent and simply washing the crude product with cold hexane (3 mL) and once with pentane (2 mL) to remove unreacted $[CpW(CO)_3]_2$ and other nonpolar species. The CH_2Cl_2-soluble portion of the remaining solid is then filtered through Celite and the CH_2Cl_2 removed in vacuo to give a yield of 70%. Spectral data for **12**: IR ν_{CO} (cm^{-1} in CH_2Cl_2) 1740 (m), 1696 (s); ^1H NMR (C_6D_6 in ppm) δ 4.30 (s, 10 H, C_5H_5), 1.47 (d, 54 H, CH_3, $^3J_{P-H} = 12$ Hz); $^{31}P\{^1H\}$ NMR (C_6D_6 in ppm) δ 85.4 (s, 2 P); MS *m*/*e* 1228 (M^+), 996 ($M^+ - {}^tBu_3P - CO$), 918 ($M^+ - 4CO - {}^tBu_3P$), 610 ($M^+ - Pd_2({}^tBu_3P)_2$).

Crystallographic Analyses. Single crystals of **9**−**12** suitable for X-ray diffraction analysis were obtained by slow evaporation of solvent from a benzene/octane solution under a slow purge of

Table 1. Crystallographic Data for Compounds 9 and 10

	9	**10**
empirical formula	$Mo_2Pt_2P_2O_4C_{38}H_{64}$	$Mo_2Pd_2P_2O_4C_{38}H_{64}$
fw	1228.89	1051.51
cryst syst	monoclinic	monoclinic
lattice params		
a (Å)	25.3036(11)	24.2769(11)
b (Å)	10.6197(5)	10.9943(5)
c (Å)	16.9923(7)	17.3532(8)
α (deg)	90	90
β (deg)	114.600(1)	116.902(1)
γ (deg)	90	90
V (Å^3)	4151.7(3)	4130.5(3)
space group	*C*2/*c*	*C*2/*c*
Z-value	4	4
ρ_{calc} (g cm^{-3})	1.966	1.691
μ(Mo Kα) (mm^{-1})	7.421	1.564
temperature (K)	294(2)	294(2)
$2\theta_{max}$ (deg)	56.56	56.66
no. of observations	4609	4652
no. of params	217	217
goodness of fit	1.065	1.070
max. shift in cycle	0.002	0.001
residuals:[a] R_1; wR_2	0.0198; 0.0482	0.0234; 0.0601
absorp corr	SADABS	SADABS
max./min.	0.522/0.394	0.925/0.740
largest peak (e Å^{-3})	1.19	0.428

[a] $R_1 = \sum_{hkl}(||F_{obs}| - |F_{calc}||)/\sum_{hkl}|F_{obs}|$; $wR_2 = [\sum_{hkl}w(|F_{obs}| - |F_{calc}|)^2/\sum_{hkl}wF^2_{obs}]^{1/2}$; $w = 1/\sigma^2(F_{obs})$; GOF $= [\sum_{hkl}w(|F_{obs}| - |F_{calc}|)^2/(n_{data} - n_{vari})]^{1/2}$.

Table 2. Crystallographic Data for Compounds 11 and 12

	11	**12**
empirical formula	$W_2Pt_2P_2O_4C_{38}H_{64}$	$W_2Pd_2P_2O_4C_{38}H_{64}$
fw	1404.71	1227.33
cryst syst	monoclinic	monoclinic
lattice params		
a (Å)	24.0266(12)	23.960(5)
b (Å)	11.1043(6)	11.018(3)
c (Å)	17.6952(9)	17.221(4)
α (deg)	90	90
β (deg)	118.510(1)	115.926(4)
γ (deg)	90	90
V (Å^3)	4148.5(4)	4088.7(16)
space group	*C*2/*c*	*C*2/*c*
Z-value	4	4
ρ_{calc} (g cm^{-3})	2.249	1.994
μ(Mo Kα) (mm^{-1})	12.364	6.589
temperature (K)	294(2)	294(2)
$2\theta_{max}$ (deg)	50.06	52.04
no. of observations	3277	3662
no. of params	203	217
goodness of fit	1.036	1.040
max. shift in cycle	0.000	0.002
residuals:[a] R_1; wR_2	0.0490; 0.1274	0.0224; 0.0547
absorp corr	SADABS	SADABS
max./min.	0.781/0.221	0.768/0.254
largest peak (e Å^{-3})	3.743	0.690

[a] $R_1 = \sum_{hkl}(||F_{obs}| - |F_{calc}||)/\sum_{hkl}|F_{obs}|$; $wR_2 = [\sum_{hkl}w(|F_{obs}| - |F_{calc}|)^2/\sum_{hkl}wF^2_{obs}]^{1/2}$; $w = 1/\sigma^2(F_{obs})$; GOF $= [\sum_{hkl}w(|F_{obs}| - |F_{calc}|)^2/(n_{data} - n_{vari})]^{1/2}$.

nitrogen at room temperature. Each data crystal was glued onto the end of a thin glass fiber. X-ray intensity data were measured by using a Bruker SMART APEX CCD-based diffractometer using Mo Kα radiation ($\lambda = 0.71073$ Å). The raw data frames were integrated with the SAINT+ program[6] by using a narrow-frame integration algorithm. Corrections for Lorentz and polarization effects were also applied with SAINT+. An empirical absorption correction based on the multiple measurement of equivalent reflections was applied using the program SADABS. All structures were solved by a combination of direct methods and difference Fourier syntheses and refined by full-matrix least-squares on F^2 using the SHELXTL software package.[7] Unless otherwise noted, all non-hydrogen atoms were refined with anisotropic displacement parameters. All hydrogen atoms were placed in geometrically idealized positions and included as standard riding atoms during the least-squares refinements. Crystal data, data collection parameters, and results of the analyses are listed in Tables 1 and 2.

All four compounds crystallized in the monoclinic crystal system and were found to have similar lattice parameters. The systematic absences in the data for each structure were consistent with the space groups *C*2/*c* and *Cc*. The former was chosen and confirmed by the successful solution and refinement of the structures. For **14**, the tri-*tert*-butylphosphine groups were disordered equally over two positions and were refined with isotropic displacement parameters.

Computational Studies. Starting coordinates for the title compounds were obtained from X-ray crystal structure data. Geometry optimizations and single-point energy calculations were performed using the Amsterdam Density Functional (ADF) program, version 2004.01, developed by Baerends et al.[8] Geometry optimizations were carried out, with C_2 symmetry restraints, using the local exchange−correlation potential of Vosko et al.[9] and the nonlocal exchange and correlation corrections of Perdew and Wang (PW91).[10] For the Pt and W atoms, the electronic configuration was described using a double-ζ Slater-type orbital (STO) basis for 5s and triple-ζ orbitals for 6s, 5p, 5d, and 4f, augmented by 6p and 5f polarization functions. The core was frozen and defined to be 4d and below. For the Mo and Pd atoms, the electronic configuration was described using a double-ζ STO basis for 4s and triple-ζ for 5s, 4p, and 4d augmented by a 5p polarization function. The core was frozen and defined to be 3d and below. For the phosphorus atoms, a triple-ζ STO basis was used for 3s and 3p. This basis was augmented with 3d and 4f polarization functions, while the core was frozen at 2p and below. For oxygen and carbon, double-ζ basis sets were employed for 2s and 2p, augmented with 3d and 4f polarization functions, and the 1s core was frozen. A double-ζ basis was used for the hydrogen atoms augmented by 2p and 3d polarization functions. Corrections for relativistic effects were employed in each calculation by using the Zeroth Order Regular Approximation (ZORA) method.[11] Accuracy and convergence parameters were left at the default level with the exception of the general integration accuracy, which was set to 7.0.

Results

The reaction of $[CpMo(CO)_3]_2$ with $Pt(PBu^t_3)_2$ and $Pd(PBu^t_3)_2$ in hexane solvent at reflux (68 °C) has yielded the new tetranuclear bimetallic cluster complexes $Cp_2Mo_2(CO)_4[M'(PBu^t_3)]_2$ [M′ = Pt (**9**) and M′ = Pd (**10**)] in 29 and 41% yields, respectively. Both compounds were characterized by IR, ^{1}H and ^{31}P NMR, and elemental and single-crystal X-ray diffraction analyses. Both compounds contain C_2 rotational symmetry within their molecular structure in the solid state. An ORTEP of the molecular structure of **9** is given in Figure 1. Selected intramolecular distances and angles are listed in Table 3. The structure of **9** has a Mo_2Pt_2 butterfly tetrahedral geometry with

(6) *SAINT+*, version 6.2a; Bruker Analytical X-ray Systems, Inc.: Madison, WI, 2001.

(7) Sheldrick, G. M. *SHELXTL*, version 6.1; Bruker Analytical X-ray Systems, Inc.: Madison, WI, 1997.

(8) (a) te Velde, G.; Bickelhaupt, F. M.; Baerends, E. J.; Fonseca-Guerra, C.; Van Gisbergen, S. J. A.; Snijdgers, J. G.; Ziegler, T. *J. Comput. Chem.* **2001**, *22*, 931. (b) Fonseca-Guerra, C.; Snijders, J. G.; te Velde, G.; Baerends, E. J. *Theor. Chem. Acc.* **1998**, *99*, 391. (c) *ADF 2004.01*; SCM, Theoretical Chemistry: Vrije Universiteit, Amsterdam, The Netherlands, http://www.scm.com.

(9) Vosko, S. H.; Wilk, L.; Nusair, M. *Can. J. Phys.* **1980**, *58*, 1200.

(10) Perdew, J. P. *Phys. Rev. B* **1992**, *46*, 6671.

(11) van Lenthe, E.; Ehlers, A. E.; Baerends, E. J. *J. Chem. Phys.* **1999**, *110*, 8943.

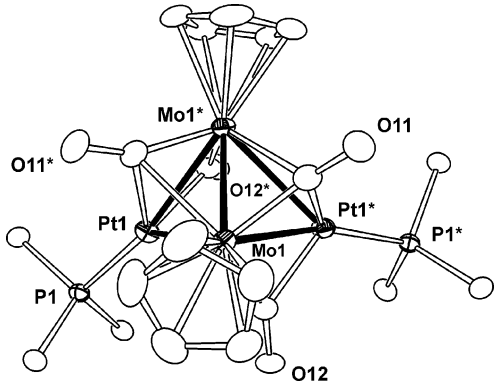

Figure 1. ORTEP of the molecular structure of $Cp_2Mo_2(CO)_4[Pt(PBu^t_3)]_2$ (**9**) showing 30% ellipsoid probability. Methyl groups on the tri-*tert*-butylphosphine ligands are omitted for clarity.

Table 3. Selected Intramolecular Distances and Angles for Compounds 9 and 11[a]

9		**11**	
	Bond Distances (Å)		
Pt(1)−Mo(1)	2.8466(3)	W(1)−Pt(1)	2.8400(6)
Pt(1)−Mo(1)*	2.7456(3)	W(1)−Pt(1)*	2.8255(6)
Mo(1)−Mo(1)*	2.6535(4)	W(1)−W(1)*	2.6168(9)
Pt(1)···Pt(1)*	3.560(1)	Pt(1)−Pt(1)*	2.9228(9)
Pt(1)−P(1)	2.3172(6)	Pt(1)−P(1)	2.312(3)
C(11)−Mo(1)	1.964(3)	C(11A)−Pt(1)	1.99(2)
C(11)−Pt(1)*	2.316(3)	C(11A)−W(1)*	2.023(19)
C(11)−Mo(1)*	2.473(3)	C(12)−W(1)	1.959(18)
C(12)−Mo(1)	2.042(3)	C−O (av)	1.19(6)
C(12)−Pt(1)*	2.034(3)		
C−O (av)	1.189(4)		
	Bond Angles (deg)		
Pt(1)−Mo(1)−Pt(1)*	79.051(7)	Pt(1)−W(1)−Pt(1)*	62.11(2)
Pt(1)−Mo(1)−Mo(1)*	59.770(7)	Pt(1)−W(1)−W(1)*	62.212(14)
Pt(1)−Mo(1)*−Mo(1)	63.609(8)	Pt(1)−W(1)*−W(1)	62.772(16)
Mo(1)−Pt(1)−Mo(1)*	56.621(9)	W(1)−Pt(1)−W(1)*	55.017(19)

[a] Estimated standard deviations in the least significant figure are given in parentheses.

the two platinum atoms occupying the "wingtip" positions. The distance between the two platinum atoms [3.560(1) Å] is too long to allow for any significant bonding interaction. Two of

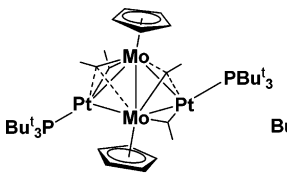

9

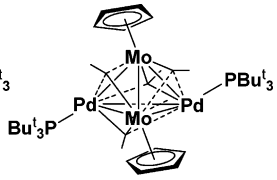

10

the carbonyl ligands symmetrically bridge opposite positioned Mo−Pt bonds [Mo(1)−C(12) = 2.042(3) Å and Pt(1)*−C(12) = 2.034(3) Å], while the other two carbonyls are semitriply bridging ligands across the two Mo_2Pt triangles [C(11)−Mo(1) = 1.964(3) Å, C(11)−Mo(1)* = 2.473(3) Å, and C(11)−Pt(1)* = 2.316(3) Å]. The Mo−Mo bond distance is quite short [2.6535(4) Å], suggesting the presence of some multiple-bond character, as will be described below. It is similar in length to the Mo−Mo "double" bond found in the compound $Cp_3Mo_2Rh(CO)_5$ [Mo−Mo = 2.654(1) Å].[12] In fact, the total valence electron count of 54 is eight electrons less than the expected number of 62 for a butterfly arrangement of four metal atoms.

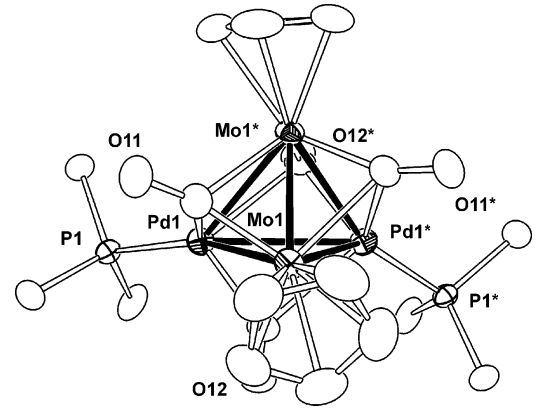

Figure 2. ORTEP of the molecular structure of $Cp_2Mo_2(CO)_4[Pd(PBu^t_3)]_2$ (**10**) showing 30% ellipsoid probability. Methyl groups on the tri-*tert*-butylphosphine ligands are omitted for clarity.

Table 4. Selected Intramolecular Distances and Angles for Compounds 10 and 12[a]

10		**12**	
	Bond Distances (Å)		
Pd(1)−Mo(1)	2.7640(2)	W(1)−Pd(1)	2.7629(5)
Pd(1)−Mo(1)*	2.8133(2)	W(1)−Pd(1)*	2.8076(5)
Mo(1)−Mo(1)*	2.6362(4)	W(1)−W(1)*	2.6320(7)
Pd(1)−Pd(1)*	3.1034(3)	Pd(1)−Pd(1)*	3.0955(9)
Pd(1)−P(1)	2.4039(5)	Pd(1)−P(1)	2.3976(10)
C(11)−Pd(1)	2.364(2)	C(12)−Pd(1)	2.386(4)
C(11)−Mo(1)	1.973(2)	C(12)−W(1)	1.953(4)
C(11)−Mo(1)*	2.411(2)	C(12)−W(1)*	2.473(4)
C(12)−Pd(1)	2.083(2)	C(11)−Pd(1)	2.085(4)
C(12)−Mo(1)	2.040(2)	C(11)−W(1)	2.015(4)
C(12)−Pd(1)*	2.612(2)	C−O (av)	1.185(7)
C−O (av)	1.177(4)		
	Bond Angles (deg)		
Pd(1)−Pd(1)*−Mo(1)	55.439(5)	Pd(1)−Pd(1)*−W(1)	55.556(10)
Pd(1)−Mo(1)−Pd(1)*	67.611(8)	Pd(1)−W(1)−Pd(1)*	67.51(2)
Pd(1)−Mo(1)−Mo(1)*	62.740(6)	Pd(1)−W(1)−W(1)*	62.665(9)
Pd(1)−Mo(1)*−Mo(1)	60.854(6)	Pd(1)−W(1)*−W(1)	60.951(12)
Mo(1)−Pd(1)−Pd(1)*	56.950(6)	W(1)−Pd(1)−Pd(1)*	56.932(12)
Mo(1)−Pd(1)−Mo(1)*	56.406(8)	W(1)−Pd(1)−W(1)*	56.384(16)

[a] Estimated standard deviations in the least significant figure are given in parentheses.

The known compound $Pt_3(CO)_3(PBu^t_3)_3$[13] was obtained as a side product in this reaction and would seem to explain the fate of the two carbonyl ligands lost from $[CpMo(CO)_3]_2$ in the course of the reaction. Even though compound **9** is highly unsaturated, attempts to add hydrogen and other small organic molecules to it were unsuccessful. It is possible that the steric crowding from the ligands around the Mo−Mo bond prevents any such addition reactions. Reaction of **9** with an excess of CO yielded $[CpMo(CO)_3]_2$ and $Pt_3(CO)_3(PBu^t_3)_3$ by degradation of the cluster.

An ORTEP of the molecular structure of **10** is given in Figure 2. Selected intramolecular bond distances and angles are listed in Table 4. Unlike in compound **9**, the metal atoms in **10** adopt a tetrahedral geometry. The Pd−Pd distance in **10** [3.1034(3) Å] is much shorter than the Pt−Pt distance in **9**; however, the Mo−Mo distance [2.6362(4) Å] is nearly identical. The structure of **10** contains four asymmetric triply bridging carbonyl ligands [e.g., C(11)−Pd(1) = 2.364(2) Å, C(11)−Mo(1) = 1.973(2) Å, and C(11)−Mo(1)* = 2.411(2) Å], one on each face of the Mo_2Pd_2 tetrahedron.

Similarly, $[CpW(CO)_3]_2$ was found to react with an excess of $M'(PBut_3)_2$ (M′ = Pt at 110 °C; M = Pd at 80 °C) to yield

(12) Winter, G.; Schulz, B.; Trunschke, A.; Miessner, H.; Bottcher, H.-C.; Walther, B. *Inorg. Chim. Acta* **1991**, *184*, 27.

(13) Goel, R. G.; Ogini, W. O.; Srivastava, R. C. *J. Organomet. Chem.* **1981**, *214*, 405.

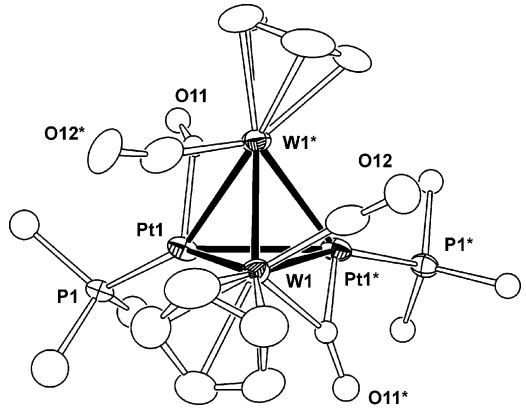

Figure 3. ORTEP of the molecular structure of $Cp_2W_2(CO)_4[Pt(PBu^t_3)]_2$ (**11**) showing 30% ellipsoid probability. Methyl groups on the tri-*tert*-butylphosphine ligands are omitted for clarity.

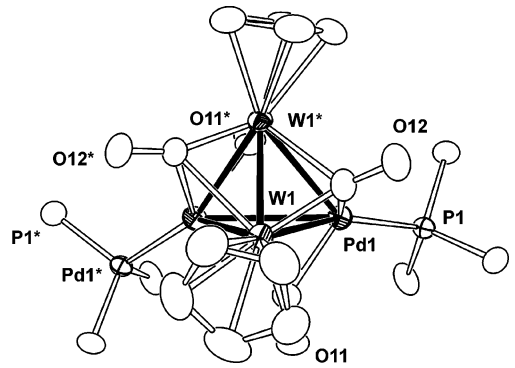

Figure 4. ORTEP of the molecular structure of $Cp_2W_2(CO)_4[Pd(PBu^t_3)]_2$ (**12**) showing 30% ellipsoid probability. Methyl groups on the tri-*tert*-butylphosphine ligands are omitted for clarity.

the new compounds $Cp_2W_2(CO)_4[M'(PBu^t_3)]_2$ [M′ = Pt (**11**) and M′ = Pd (**12**)] in 18 and 22% yields, respectively. Both compounds were characterized by IR, ^{1}H and ^{31}P NMR, and elemental and single-crystal X-ray diffraction analyses. ORTEP diagrams of the molecular structures of **11** and **12** are given in Figures 3 and 4, respectively; selected intramolecular distances and angles are listed in Tables 3 and 4.

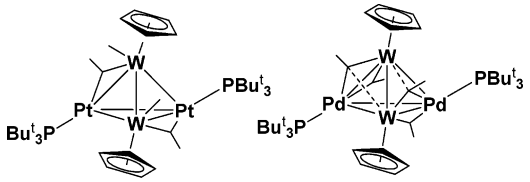

Both compounds are centrosymmetrical in the solid state. The structure of **11** consists of a W_2Pt_2 tetrahedron with two terminal carbonyl ligands on W(1) and W(1)* and two bridging carbonyl ligands on the W(1)−Pt(1)* and W(1)*−Pt(1) bonds. The W−W distance [2.6168(9) Å] is similar to the Mo−Mo distances in **9** and **10**, but the Pt−Pt distance [2.9228(9) Å] is much shorter than found in **9**. The metal atoms in **12** are similarly positioned in a tetrahedral-like arrangement. Two carbonyl ligands symmetrically bridge the Pd(1)−W(1) and Pd(1)*−W(1)* bonds, while the other two are semitriply bridging the W(1)−W(1)*−Pd(1) and W(1)−W(1)*−Pd(1)* triangles. The W−W [2.6320(7) Å] and the Pd−Pd [3.0955(9) Å] distances are similar to those found in **10**. The total valence electron count for compounds **10**−**12** is 54 and is still six electrons less than the expected number of 60 for a tetrahedral arrangement of four metal atoms. However, if the M−M (M = Mo, W) interaction is counted as a double bond, each Mo or W atom achieves an 18-electron configuration, while each Pd or Pt atom could be viewed as stable with 16-electron configurations.

A number of years ago, Braunstein and co-workers synthesized bis(cyclopentadienyl)bis(phosphine)tetranuclear metal complexes containing six carbonyl ligands, two group VI metal atoms, and either two platinum or two palladium atoms: $Cp_2M_2M'_2(CO)_6(PR_3)_2$ (Cp = C_5H_5; M = Cr, Mo, W; M′ = Pt, Pd; R = Me, Et, Bu^n, Ph).[14] Two isomeric structures for these compounds were established. The compound $Cp_2Mo_2Pt_2(CO)_6(PEt_3)_2$ (**13**) exhibits a planar Mo_2Pt_2 butterfly cluster with two platinum atoms occupying the "hinge" positions and two molybdenum atoms at the "wingtip" positions. Four of the six carbonyl ligands asymmetrically bridge each of the Mo−Pt bonds of the cluster; the other two carbonyls were described as semitriply bridging carbonyl ligands spanning the two Pt−Mo−Pt triangles. With bulkier phosphine ligands (e.g., PCy_3 and PPr^i_3) two skeletal isomers were formed that could be interconverted in solution.[15] For example, the compound $Cp_2Mo_2Pt_2(CO)_6(PCy_3)_2$ (**14**) (Cp = C_5H_4Me) exists as a mixture of two isomers: one with a planar geometry similar to **13** and another that contains a tetrahedral configuration of metal atoms (**14**).

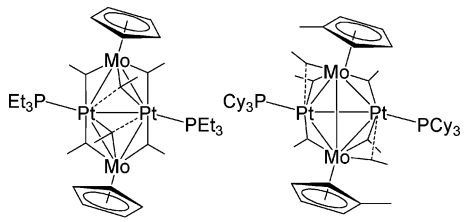

It is probable that the bulk of the tri-*tert*-butlyphosphine ligands in **9**−**12** causes the metal atoms to adopt only the tetrahedral arrangement similar to **14**, as opposed to a planar arrangement similar to **13**. In fact, the crowded nature of the ligands around the metal core may make it impossible for even the smallest of molecules to add to these unsaturated compounds. Indeed in their synthesis, two carbonyls are lost and subsequently scavenged by the excess $M'(PBu^t_3)_2$ (M′ = Pt, Pd) in solution.

Computational Results

DFT studies on compounds **9** and **10** were undertaken in order to answer several questions. First, how do the Pd(Bu$^t_3$P) and Pt(Bu$^t_3$P) fragments bond to the dimolybdenum unit? Second, what is the nature of the Mo−Mo bond within the tetranuclear clusters? Namely, is there any theoretical evidence of multiple bonding between these atoms? Third, is there an explanation for the difference in the long Pt−Pt bond distance in **9** and the much shorter Pd−Pd distance found for **10**?

Mo−Pd Bonding in Cluster 10. A fragment molecular orbital (FMO) approach was used to analyze the bonding between two Mo atoms and the two Pd atoms in **10** (Figure 5). Compound **10** is viewed here as the combination of two

(14) (a) Bender, R.; Braunstein, P.; Jud, J.-M.; Dusausoy, Y. *Inorg. Chem.* **1983**, *22*, 3394. (b) Bender, R.; Braunstein, P.; Jud, J.-M.; Dusausoy, Y. *Inorg. Chem.* **1984**, *23*, 4489.

(15) Braunstein, P.; Bellefon, C. M.; Bouaoud, S.-E.; Grandjean, D.; Halet, J.-F.; Saillard, J.-Y. *J. Am. Chem. Soc.* **1991**, *113*, 5282.

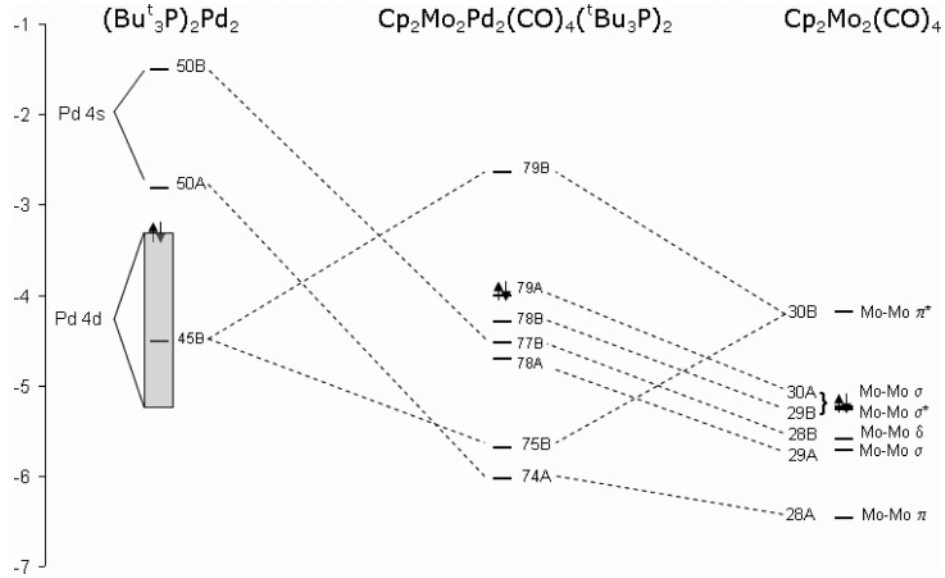

Figure 5. FMO analysis of the bonding in **10**. Energies are in units of eV.

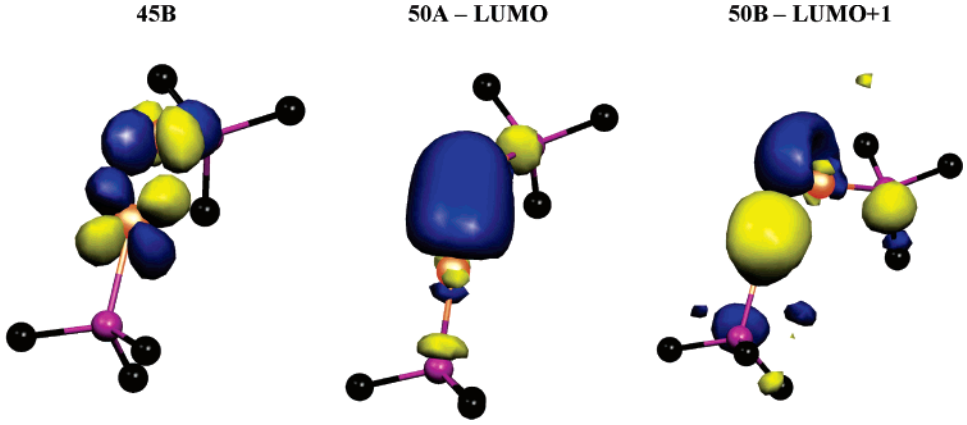

Figure 6. Selected FMOs for the $Pd_2(Bu^t_3P)_2$ fragment.

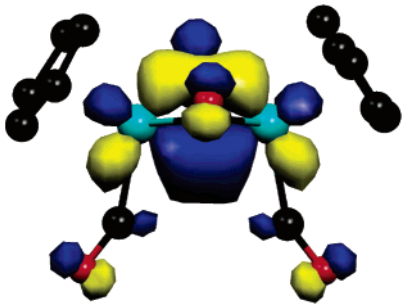

Figure 7. FMO 28A for the $Cp_2Mo_2(CO)_4$ fragment.

fragments: $Cp_2Mo_2(CO)_4$ (Figure 5, right) and (Bu^t_3P)Pd−Pd-(PBu^t_3) (Figure 5, left). The fragment electronic structures were obtained from single point energy (SPE) calculations without geometry optimization on the fragment coordinates obtained from a calculation giving a converged geometry for the complete molecule of **10**. The ADF program then allows that the fragment MOs may be used as the basis input, instead of atomic basis sets, for a subsequent SPE calculation on the entire molecule. Three of the fragment orbitals that were calculated for the Pd_2 unit were found to be particularly important for interacting with the Mo_2 fragment (Figure 6). The first of these is filled FMO 45B, which is comprised of the symmetric combination of two Pd 4d (*xy*-like) orbitals that are arranged in a Pd−Pd π-bonding symmetry. This orbital is found buried within a set of other nonbonding orbitals that are almost entirely Pd 4(d) in character (see Figure 5, left). The LUMO and LUMO+1 of the Pd_2 fragment are also involved in bonding with filled orbitals from the Mo_2 fragment. These two FMOs, 50A and 50B, respectively, are the symmetric and antisymmetric combinations of hybrids consisting of Pd 5s and Pd 5p atomic orbitals (Figure 6).

The highest energy, occupied FMOs calculated for the Mo_2 fragment are 28A, 29A, 28B, 29B, and 30A (Figure 5, right, and Figures 7−9). The bonding within these orbitals can be qualitatively described as follows. FMO 28A is Mo−Mo π-bonding in character and shows the strongest Mo−Mo overlap (Figure 7). FMO 29A also exhibits Mo−Mo overlap of σ-symmetry that is effectively negated by a Mo−Mo bonding of σ*-symmetry found in FMO 29B (Figure 8). Both FMO 29A and FMO 29B also show significant Mo to carbonyl carbon back-bonding interactions with the μ_2-carbonyl ligands bridging the Mo atoms. The two remaining occupied FMOs are 28B, which is of Mo−Mo δ-bonding symmetry, and 30A, which appears to be a weak Mo−Mo σ-interaction between the taurii of two d_{z^2}-like Mo 4d hybrid orbitals (Figure 9). The LUMO of the Mo fragment, FMO 30B, is Mo−Mo π* in character (Figure 10). The bonding in the Mo_2 fragment can be construed formally as Mo−Mo triple bond-like, which should be slightly weaker than the triple bond found for the known molecule $[CpMo(CO)_2]_2$, which has a different conformation for the ligands and probably better Mo−Mo overlap.[16]

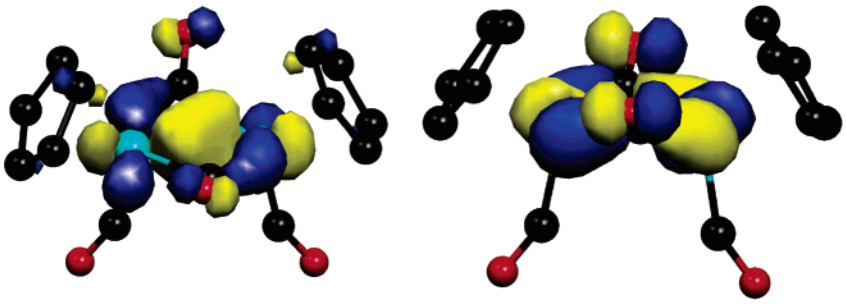

Figure 8. FMOs 29A (left) and 29B (right) for the $Cp_2Mo_2(CO)_4$ fragment.

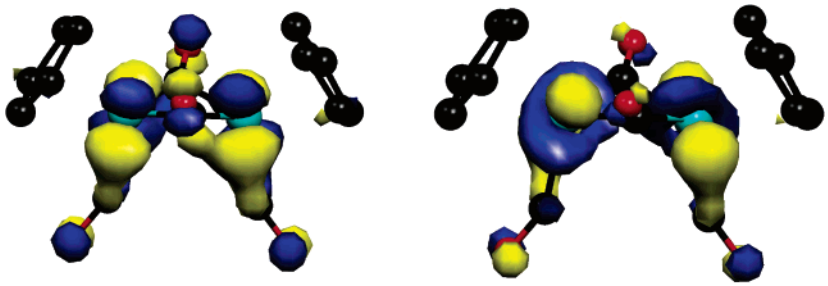

Figure 9. FMOs 28B (left) and 30A (HOMO, right) for the $Cp_2Mo_2(CO)_4$ fragment.

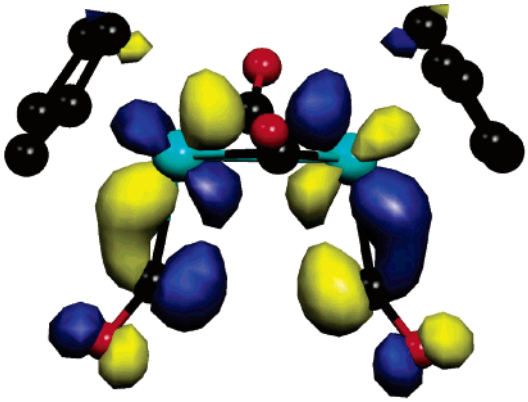

Figure 10. FMO 30B, LUMO for the $Cp_2Mo_2(CO)_4$ fragment.

When the Mo_2 and Pd_2 fragments are brought together, the dimolybdenum FMO 28A, which is Mo−Mo π-bonding in character, finds a good symmetry match with the unfilled dipalladium FMO 50A to form cluster MO 74A, which exhibits strong Mo−Pd bonding (Figure 5 and Table 5, top). Dimolybdenum FMO 28B, which is Mo−Mo δ-bonding in character, finds a match with unfilled dipalladium FMO 50B to give the second Mo−Pd bonding interaction in cluster MO 77B (Figure 5 and Table 5, bottom). There is also significant interaction between the filled Pd_2 FMO 45B, which consists of a symmetrical π-interaction between two Pd 4d (*xy*-like) atomic orbitals and the unfilled Mo_2 fragment LUMO, 30B, of Mo−Mo π* symmetry. This interaction gives rise to the formation of cluster MOs 75B (Mo−Pd bonding) and 79B (Mo−Pd antibonding) (Figure 5 and Table 6). It is clear that the bonding interaction in 75B occurs mostly through interactions between Pd and carbon atoms of the carbonyl ligands bridging the Mo−Pd vector and does not contribute greatly to the overall bonding between the Mo and Pd atoms.

Mo−Mo Bonding in Cluster 10. The degree of Mo−Mo bonding in cluster **10** can be qualitatively estimated by analyzing the filled cluster MOs that are predominantly Mo in character. Pictures for cluster MOs 74A, 75B, 78A, 77B, 78B, and 79A are presented in Figure 11. The Mo−Mo bonding in orbitals 74A and 75B appears to offset to some degree as both the Mo−Mo π and π* interactions are employed in bonding to the Pd_2 fragment. The strong Mo−Mo σ-bonding in orbital 78A also appears to be neutralized by the Mo−Mo bonding of σ* symmetry in orbital 78B. The Mo−Mo δ-bond (seen in orbital 77B) is also partially removed by bonding to Pd_2. Therefore, the majority of the Mo−Mo bonding for cluster **10** occurs as a result of the Mo−Mo bonding found in orbital 79A. The weak Mo−Mo σ-bond found in the cluster HOMO, orbital 79A, does not appear to be perturbed by interactions with Pd_2.

An absolute quantification of the Mo−Mo bond order in **10** is difficult since there are varying degrees to which bonding and antibonding counterparts (such as 74A and 74B) might cancel each other with respect to Mo−Mo bonding. This is also obscured by interactions with the bridging CO ligands. Significant interactions from the bridging CO were also found in the Mo−Mo bonding of the parent molecule $[CpMo(CO)_2]_2$.[17] Orbital 75B is mostly Pd in character; therefore the majority of the Mo−Mo π* character is found in the unfilled cluster LUMO 79B and not in the filled cluster MO 75B. It is therefore unlikely that all of the Mo−Mo π interaction in orbital 74A is canceled by the Mo−Mo π* in 75B. In cluster **10** there exists at least one weak Mo−Mo σ-bond (74A) and probably close to two Mo−Mo bonds due to the incomplete loss of the Mo−Mo π interaction. In analyzing the MO picture for cluster **10**, it appears that one of these Mo−Mo bonds becomes neutralized upon binding to Pd−PR_3. Overall, the formulation of the Mo−Mo bond formally as double seems to be reasonable for **10**. Suffice it to say, there is certainly unsaturation in the immediate vicinity of the Mo−Mo and W−W bonds in **9**−**12**. This is consistent with the short M−M distances observed in each of these compounds **10**.

Pt−Pt Interactions in Cluster 9. Two geometry optimizations on Pt cluster **9** resulted in the calculation of two different energy minima depending on the starting coordinates that were

(16) (a) Jemmis, E. D.; Pinhas, A. R.; Hoffmann, R. *J. Am. Chem. Soc.* **1980**, *102*, 2576. (b) Klingler, R. J.; Butler, W.; Curtis, M. D. *J. Am. Chem. Soc.* **1975**, *97* (12), 3535.

(17) Morris-Sherwood, B. J.; Powell, C. B.; Hall, M. B. *J. Am. Chem. Soc.* **1984**, *106*, 5079.

Table 5. Mo−Pd Interactions between Filled Mo_2 FMOs and Unfilled Pd_2 FMOs

Mo_2 FMO	Pd_2 FMO	Cluster MO
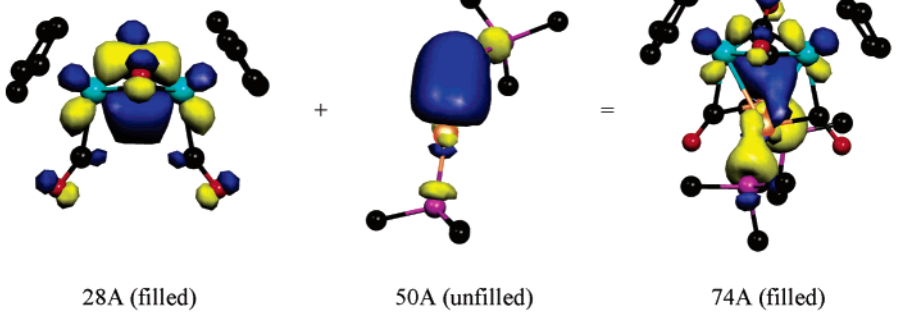		
28A (filled)	50A (unfilled)	74A (filled)
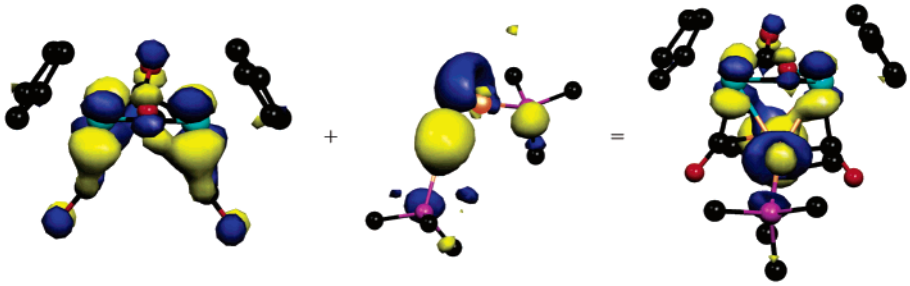		
28B (filled)	50B (unfilled)	77B (filled)

Table 6. Bonding and Antibonding Interactions between the LUMO of the Mo_2 Fragment and Pd_2 FMO 30B

Mo_2 FMO	Pd_2 FMO	Cluster MO
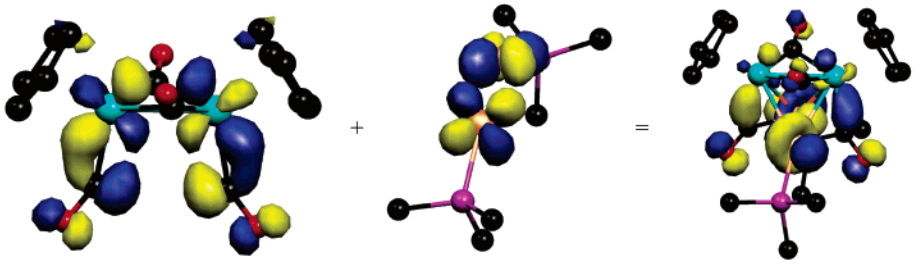		
45B (unfilled)	30B (filled)	75B (filled)
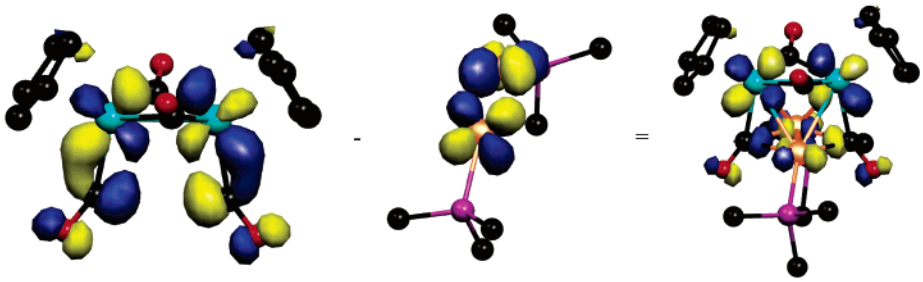		
45B (unfilled)	30B (filled)	79B (unfilled)

used. When the starting Pt−Pt bond distance was set at ca. 3.100 Å, the Pt−Pt distance in the optimized structure was 3.147 Å. However, when the starting Pt−Pt distance was set at the experimental bond distance of 3.560 Å, the distance in the optimized structure was 3.590 Å. The difference in total bonding energy between these two optimized structures, as calculated by ADF, was only about 2 kcal/mol, with the isomer having the long Pt−Pt distance being slightly lower in energy. This suggests that there is no appreciable lowering of energy by moving the Pt atoms closer to each other, and in fact, it is likely

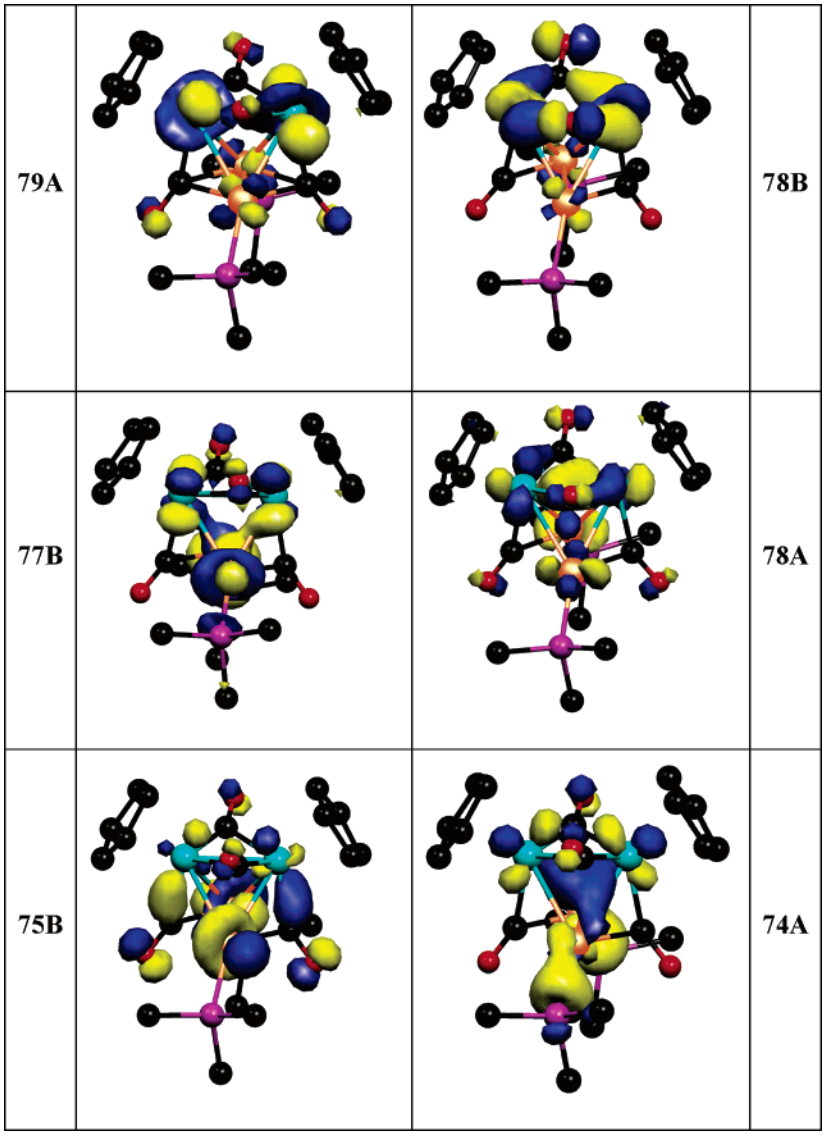

Figure 11. Selected MO pictures for **10**.

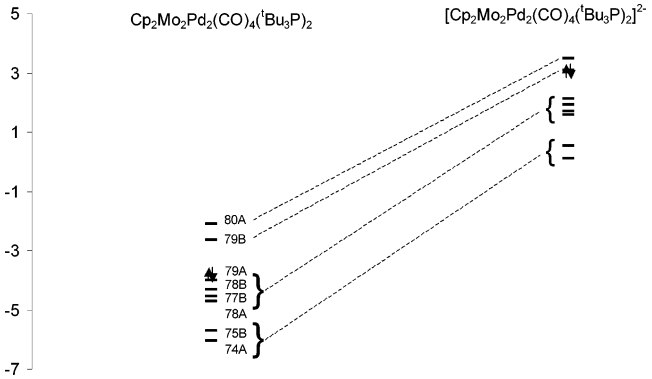

Figure 12. Correlation diagram for **10** and $[\mathbf{10}]^{2-}$. Energies are in units of eV.

that the structure with the short Pt−Pt interaction is actually disfavored by nonbonded Pt−Pt repulsions, as observed experimentally. An analysis of the calculated cluster MOs for compounds **9** and **10** revealed that there are no orbitals having significant Pd−Pd or Pt−Pt bonds that are not canceled by antibonding counterparts. There are only slight differences in the energies of the MOs calculated for the long and short bond geometries calculated for cluster **9**. The small difference in energy calculated for the long and short bond structures of **9** suggests that Pd−Pd and Pt−Pt bonding is minimal. The Pt and Pd atoms in clusters **10**−**12** may exhibit shorter distances than expected simply due to steric effects from the ligands.

Computational Study of $[\mathbf{10}]^{2-}$. A computational study of the hypothetical two-electron-reduced anion, $[Cp_2Mo_2Pd_2(CO)_4(Bu^t{}_3P)_2]^{2-}$ $[\mathbf{10}]^{2-}$, was performed and revealed that, as expected, two electrons fill the LUMO of Mo−Mo π^* symmetry calculated for **10** with little change in the remaining MOs (Figure 12). An elongation of the calculated Mo−Mo bond distance from 2.647 Å to 2.833 Å is produced as a result of the addition of two electrons to **10**. It is evident from this analysis that reduction of **10** with a reagent such as H_2 might lead to addition at the Mo_2 unit and subsequent elongation of the Mo−Mo bond distance, rather than addition at one or both of the Pd or Pt atoms. Efforts to verify the feasibility of this reduction experimentally were made by cyclic voltammetry measurements in acetonitrile solvent, but no redox processes were observed in the range +2.00 to −2.00 V.

Acknowledgment. This research was supported by the Office of Basic Energy Sciences of the U.S. Department of Energy under Grant No. DE-FG02-00ER14980. We also thank the Ohio Supercomputing Center (www.osc.edu) and Prof.

Malcolm H. Chisholm at The Ohio State University for a generous grant of computational time on the IA32 Pentium 4 cluster.

Supporting Information Available: CIF files are available for each of the structural analyses and calculated Cartesian coordinates, selected bond distances, and selected bond angles for DFT-optimized structures of **9**−**12** as well as for the dianion [**10**]$^{2-}$. This material is available free of charge via the Internet at http://pubs.acs.org.

OM060107G